# Interplay between Aryl···Perfluoroaryl and Hydrogen Bonding Interactions in Cocrystals of Pentafluorophenol with Molecules of Trigonal Symmetry

Jan Alfuth, Jarosław Chojnacki, Tadeusz Połoński, Aleksander Herman, Maria J. Milewska, and Teresa Olszewska*
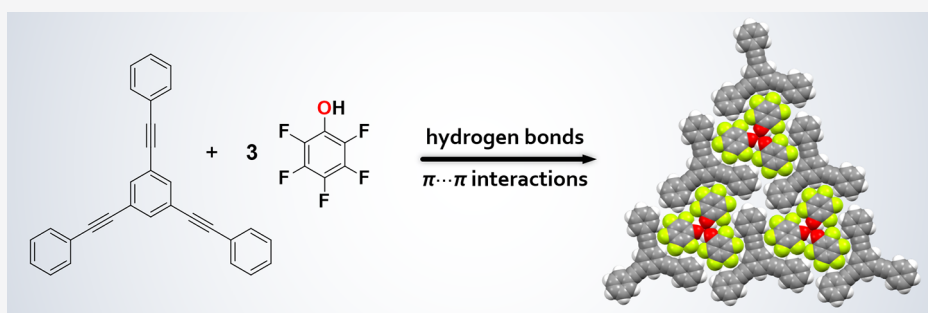
ACCESS | Metrics & More | Article Recommendations | SI Supporting Information

**ABSTRACT:** Cocrystals of seven star-shaped triaryl compounds with pentafluorophenol (**pfp**) were prepared and structurally characterized by the single-crystal X-ray diffraction method. Cocrystallization of **pfp** with planar (or almost planar) compounds gave six 3:1 molecular complexes with well-defined layered structures. The layers are composed of alternating **pfp**$_3$ trimers, linked by hydrogen bonding, and triaryl molecules held together in planes by the weak C−H···F interactions. Stacking interactions of the triaryl-substituted molecules with the perfluorinated rings of **pfp** are responsible for the overall crystal packing, but most likely also stabilize the trimers in the solid state, as the assembly of the **pfp** into trimers provide an optimal geometry for the $\pi$···$\pi$ interaction. The layers are flat for the cases of components with almost planar geometry and corrugated for those with more twisted geometry. In the case of nonplanar triphenyl isocyanurate, the **pfp** cocrystal does not contain **pfp**$_3$ trimers, the stoichiometry changes from 3:1 to 3:2 (3 refers to **pfp**), and the packing is mainly controlled by intermolecular O−H···O=C hydrogen bonding.

## INTRODUCTION

Aromatic $\pi$···$\pi$ interactions play an important role in supramolecular chemistry, biology, and materials science.[1−6] They are responsible for DNA base stacking,[7] intercalation of drugs with DNA,[8] protein folding,[9] and molecular recognition.[1,2] Stacking interactions are commonly used to organize molecular assemblies in crystalline solids[10] or liquid crystalline[11] phases and are critical for the design of new functional materials.[12] In comparison with typical non-covalent interactions such as hydrogen bonds (HBs) or metal coordination, the interactions between aromatic rings are rather weak (calculated intermolecular forces between two stacked benzene rings are of the order of −2 kcal/mol).[13−15] On the other hand, offset face-to-face aryl···perfluoroaryl forces are approximately twice as attractive as analogous homoaromatic interactions.[15,16] It can be attributed to a quadrupolar interaction between electron-rich and electron-deficient aromatic systems.[2,17,18] However, detailed calculations show that dispersion interactions and solvophobic effects are equally important.[2,6] Thus, arenes and perfluoroarenes can cocrystallize in molecular complexes that show a stacked structure with an alternate sequence of component molecules,[19]

while pure components, particularly those with smaller ring systems, usually prefer to crystallize in an edge-to-face mode.[20] The crystallographic investigations performed in recent two decades have provided numerous examples of ordered binary complexes with aryl···perfluoroaryl structure and this interaction has emerged as an important synthon in crystal engineering that can be used to control the relative orientation of molecules toward each other.[21−23] However, most of these studies have dealt with cocrystals of hydrocarbons and perfluorocarbons[24−26] and only a few studies have described cocrystals of compounds bearing functional groups.[27−33] Particularly, pentafluorophenol (**pfp**) seems to have a potential as a versatile component for the construction of ordered supramolecular crystalline assemblies
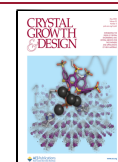
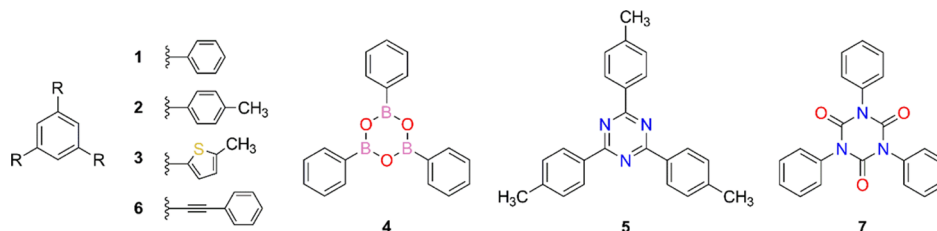**Scheme 1. Chemical Structures of the Hydrogen-Bonded Aggregates of Alcohols and Phenols I−III, pfp and pfp$_3$**
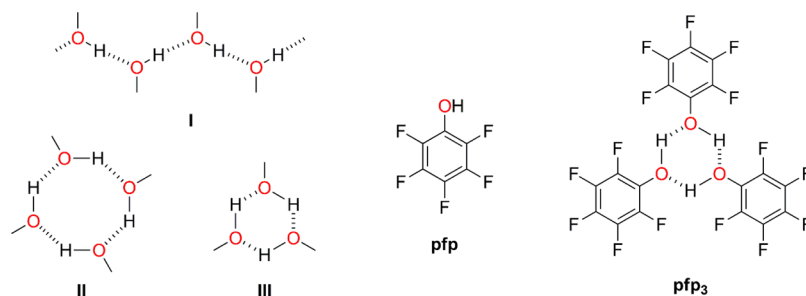


**Scheme 2. Chemical Structures of Components 1−7 Used in the Study**

where the interplay of hydrogen bonding and aryl···perfluoroaryl interactions opens possibility to control their architecture in a predictable way.[34−36]

Because hydroxyl groups may act both as donors and acceptors of HB, in the solid state, alcohols and phenols form several types of hydrogen-bonded O−H···O aggregates such as chains or rings (**I−III**) (Scheme 1).[37] In the graph set notation, those motifs can be described as C(3), $R_4^4(8)$ and $R_3^3(8)$ for **I**, **II**, and **III**, respectively.

Due to its symmetry, the six-membered ring (**III**) seems to be a particularly attractive synthon in crystal engineering.[38] Our inspection of the Cambridge Structural Database (CSD v. 5.42, updates Feb. 2022) has revealed 73 structures in which the motif **III** is present in substituted phenols. However, most of the structures contain preorganized phenol units, either by macrocyclic structures such as calixarenes[39] or homocalixarenes[40] or by complexation to metal centers.[41] The only two examples of simple phenol structures containing the synthon **III**: 2,3-dichlorophenol and 2,3,4-trichlorophenol MeOH solvate, have been reported by Desiraju and coworkers.[42] Pure phenol (PhOH) forms two polymorphic structures which are characterized by HB helical chains differing in conformation adopted by PhOH molecules.[43,44] Similarly, three polymorphs of **pfp** are known: two more stable, forming infinite O−H···O−H···O−H chains and a less stable one, consisting of discrete linear trimers connected by O−H···F−C bridges.[45−47] On the other hand, phenol and **pfp** form cocrystals where alternating PhOH and **pfp** molecules form stacks with intermolecular O−H···O hydrogen bonding between them.[34]

We expected that cocrystallization of **pfp** with suitable compounds of trigonal symmetry (Scheme 2) should force a formation of hydrogen-bond-stabilized pentafluorophenol trimers (**pfp$_3$**) due to the stacking aryl···perfluoroaryl interactions between the components. Furthermore, the usage of the substrates with high symmetry may lead to aesthetically appealing crystal structures with the anticipation of the transfer of molecular symmetry to supramolecular symmetry.[48−50] Thus, we have chosen triarylbenzenes **1−3**, triphenylboroxine (**4**), 2,4,6-tris(4-methylphenyl)-1,3,5-triazine (**5**), 1,3,5-tris-(phenylethynyl)benzene (**6**), and 1,3,5-triphenylisocyanurate

(**7**), that is, molecules with a topological $C_3$-symmetry, as components for cocrystallization with **pfp** and described the crystal structures of the resulted molecular complexes. In the next step, we used Hirshfeld surface (HS) analysis to demonstrate intermolecular interactions and assess intercontact distributions.[51,52]

## EXPERIMENTAL METHODS

**Synthesis and Crystallization.** Commercially available chemicals were used without any purification. Solvents were dried following the standard procedures. Compounds **1−7** were obtained according to the literature procedures. 1,3,5-Triarylbenzenes **1−3** were obtained by cyclotrimerization of corresponding aryl-methyl ketones mediated by SOCl$_2$−EtOH.[53,54] Triphenylboroxine (**4**) was prepared by the dehydration of phenylboronic acid in a presence of SOCl$_2$.[55] 2,4,6-Tris(4-methylphenyl)-1,3,5-triazine (**5**) was prepared by the acid-catalyzed trimerization of $p$-tolunitrile.[56] 1,3,5-Tris(phenylethynyl)-benzene (**6**) was synthesized by Sonogashira coupling of 1,3,5-tribromobenzene with phenylacetylene.[57] 1,3,5-Triphenylisocyanurate (**7**) was obtained by catalytic trimerization of phenyl isocyanate.[58] Single crystals of the complexes were grown by slow evaporation of heptane−CH$_2$Cl$_2$ solution of the corresponding substrate with a molar excess of **pfp**. Colorless crystals of the complexes are not air-stable and slowly decompose due to volatility of **pfp**. However, they can be stored for a long time in the mother liquor or in the presence of **pfp** vapor.

**Theoretical Calculations.** The geometry optimizations of the isolated molecules of hexafluorobenzene, **pfp** and **1−7** at the HF/6-311G* level of theory and calculations of molecular electrostatic potentials (MEPs) were carried out using FireFly[59,60] and MaSK[61] packages.

The HSs and fingerprint plots were generated using the CrystalExplorer17 program.[62] In the case of **2·pfp$_3$**, one orientation of the methyl group laying on the twofold rotation axis and one orientation of the OH groups in the **pfp$_3$** trimer were chosen and modeled as fully occupied and then the HS was calculated. HSs of both molecules of **6** and both **pfp$_3$** trimers in **6·pfp$_3$** are almost the same and give almost identical fingerprint plots (see the Supporting Information); therefore, one of each was chosen and presented.

**X-ray Diffraction.** Diffraction intensities data were collected on an IPDS 2T dual beam diffractometer (STOE & Cie GmbH, Darmstadt, Germany) at 120.0(2) K with Mo Kα radiation of a microfocus X-ray source (GeniX 3D Mo High Flux, Xenocs, Sassenage, 50 kV, 1.0 mA, and λ = 0.71069 Å). The investigated crystals were thermostated under
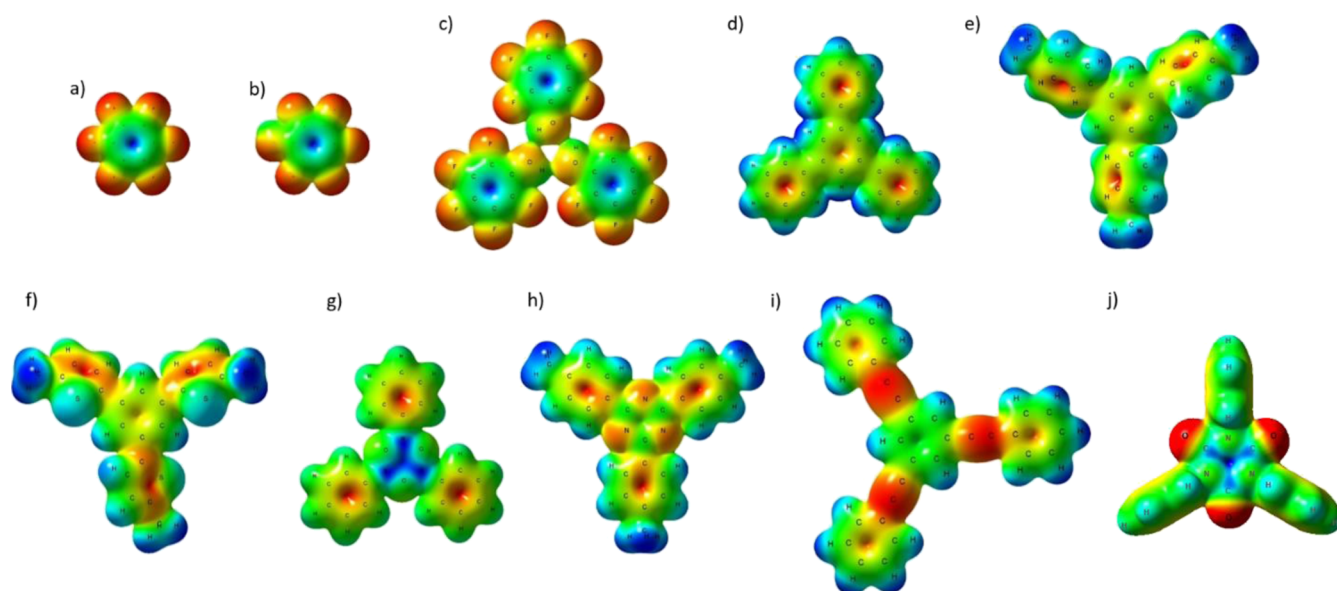
**Figure 1.** Molecular electrostatic potential of the following: (a) hexafluorobenzene; (b) **pfp**; (c) **pfp₃** trimer; (d) **1**; (e) **2**; (f) **3**; (g) **4**; (h) **5**; (i) **6**; and (j) **7**, computed at the HF/6-311G* level of theory, mapped on 0.01 Å⁻³ electron density surface.

**Table 1. Parameters of the O−H⋯O HBs in Cocrystals 1·pfp₃−6·pfp₃ and O−H⋯O═C HBs in 7·pfp[a]**

| cocrystal | interaction | $d_{O-H}$ (Å) | $d_{H\cdots O}$ (Å) | $d_{O\cdots O}$ (Å) | $\theta_{O-H\cdots O}$ (deg) |
|---|---|---|---|---|---|
| **1·pfp₃** | O1−H1⋯O2 | 0.85(2) | 2.15(8) | 2.727(7) | 125(8) |
| | O2−H2⋯O3 | 0.84 | 2.03 | 2.730(7) | 140 |
| | O3−H3⋯O1 | 0.85(2) | 2.04(7) | 2.701(7) | 134(8) |
| **2·pfp₃** | O1−H1A⋯O2 | 0.84 | 2.41 | 2.740(3) | 104 |
| | O2−H2⋯O1[b] | 0.84(2) | 2.18(6) | 2.740(3) | 124(6) |
| | O1−H1B⋯O1[b] | 0.82(2) | 2.09(4) | 2.795(4) | 143(6) |
| **3·pfp₃** | O2−H2⋯O3 | 0.84(2) | 2.10(7) | 2.718(7) | 130(8) |
| | O3−H3⋯O1 | 0.84(2) | 2.09(8) | 2.746(7) | 135(9) |
| | O1−H1⋯O2 | 0.84(2) | 2.01(6) | 2.740(7) | 146(9) |
| **4·pfp₃** | O1−H1⋯O2 | 0.80(2) | 2.16(4) | 2.713(4) | 127(4) |
| | O3−H3⋯O1 | 0.80(2) | 2.14(4) | 2.723(4) | 130(4) |
| | O2−H2⋯O3 | 0.82(2) | 2.04(3) | 2.770(4) | 148(4) |
| **5·pfp₃** | O3−H3⋯N1 | 0.84 | 2.59 | 3.419(15) | 168 |
| | O2−H2⋯O3 | 0.84 | 2.20 | 2.781(12) | 127 |
| | O1−H1⋯O2 | 0.84 | 2.21 | 2.720(16) | 119 |
| **6·pfp₃** | O1−H1⋯O2 | 0.83(3) | 2.02(4) | 2.716(5) | 141(5) |
| | O2−H2⋯O3 | 0.84 | 2.11 | 2.683(4) | 126 |
| | O3−H3⋯O1 | 0.84 | 2.09 | 2.681(5) | 127 |
| | O4−H4⋯O6 | 0.84 | 2.10 | 2.692(4) | 128 |
| | O5−H5⋯O4 | 0.84 | 2.09 | 2.689(4) | 128 |
| | O6−H6⋯O5 | 0.85(3) | 1.94(5) | 2.686(4) | 147(7) |
| **7·pfp** | O1−H1⋯O4 | 0.85(3) | 1.90(3) | 2.734(3) | 166(4) |
| | O2−H2⋯O6 | 0.83(3) | 1.95(3) | 2.751(3) | 162(6) |
| | O3−H3⋯O7 | 0.84(3) | 1.89(3) | 2.692(3) | 160(5) |

[a]For **5·pfp₃**, one O−H⋯N contact instead of O−H⋯O interaction is reported. [b]Symmetry code: −x + 1.5, y, −z + 1.5.

a nitrogen stream at 120 K using the Cryostream-800 device (Oxford CryoSystem, UK) during the entire experiment. For details see the Supporting Information. Crystal data, data collection, and structure refinement details are summarized in Table S1.

## ■ RESULTS AND DISCUSSION

**Molecular Electrostatic Potential Maps.** MEP mapped onto van der Waals surfaces is a useful qualitative guide in analysis of the electron-deficient ($\pi$-acidic) or -rich ($\pi$-basic) regions and prediction of intermolecular interactions.[63] The negative and positive potentials depicted as red and blue areas

on color plots (Figure 1) correspond to electron-rich and electron-deficient regions, respectively. Aromatic rings with large positive quadrupole moments perpendicular to the ring plane $Q_{ZZ}$ (expressed in Buckinghams, B) can participate in stacking interaction with the rings bearing negative $Q_{ZZ}$ values. The OH substituent in **pfp** slightly reduces the MEP at the ring center compared to hexafluorobenzene as shown by the $Q_{ZZ}$ values of 6.45 and 10.02 B, respectively (Figure 1a,b). On the other hand, the HBs in the **pfp₃** trimers **III** do not significantly influence the MEP surfaces of $\pi$-acidic pentafluorophenyl units (Figure 1c). Inspection of the MEP plots of triaryl compounds
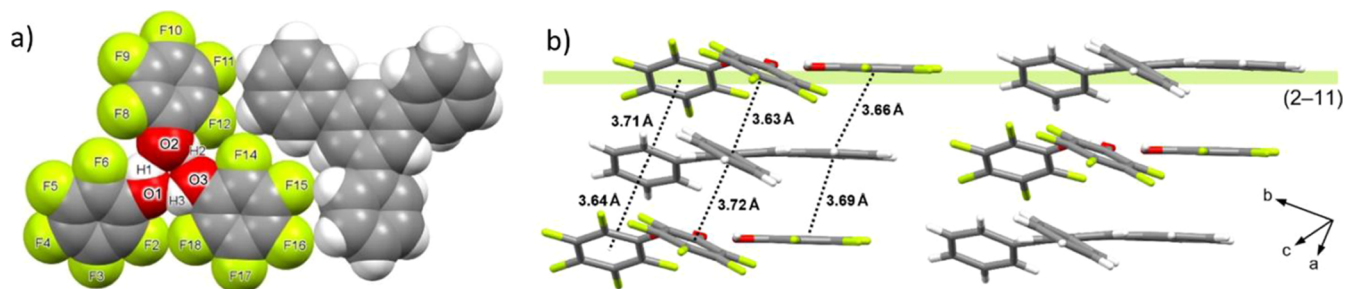
**Figure 2.** Crystal structure of **1·pfp**₃: (a) view of the **pfp**₃ trimer and the molecule of **1** with numbering of the OH groups and F atoms; (b) projection along the layers with Miller index of a family of parallel planes with the same orientation together with distances between centroids of the interacting rings (dotted lines).



**Figure 3.** Crystal structure of **2·pfp**₃: (a) view of the **pfp**₃ trimer and the molecule of **2** with numbering of the OH groups and F atoms; (b) projection along the layers with the Miller index of a family of parallel planes with the same orientation together with distances between centroids of the interacting rings (dotted lines).
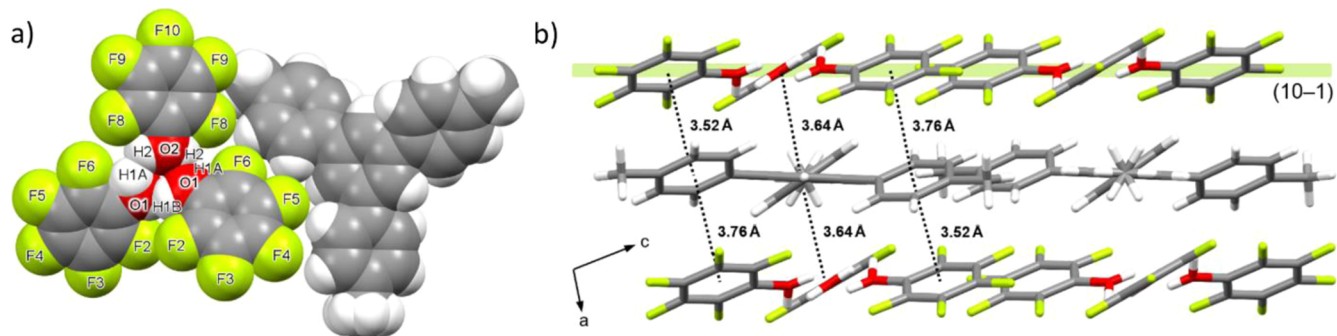
**1**−**7** clearly indicates that all phenyl or *p*-tolyl units connected to the central ring are π-basic as indicated by red MEP surfaces at their centers (Figure 1d−j). Analogously, the central aryl rings in the molecules of **1**−**3** are π-basic. In contrast, the boroxine ring in **4** at the boron atom region (Figure 1g) and the central ring in **7** (Figure 1j) show marked π-acidic character. Similarly, the central benzene unit in **6** remains slightly acidic; however, in this case three ethynyl moieties exert highly negative (red) contribution (Figure 1i).

**Crystal Structures.** The first choice of a coformer with a topological $C_3$-symmetry was naturally 1,3,5-triphenylbenzene (**1**) being the simplest and having the right shape and dimensions similar to the **pfp**₃ trimer. Then, 2,4,6-tris(*p*-tolyl)benzene (**2**) was tested to check whether enlarging the component size by three methyl groups influences the formation of the trimers. In both cases, the cocrystallization was successful and the 1,3,5-triarylbenzenes formed 1:3 complexes. However, these molecules are significantly distorted from planarity due to steric interactions between neighboring hydrogen atoms of the central benzene unit and the aryl substituents. As a consequence of the aryl···perfluoroaryl stacking interactions, the geometry of the **pfp**₃ trimers in the corresponding cocrystals closely follows that of **1** or **2**. Parameters for HBs of the trimers are presented in Table 1. Numerous C−H···F interactions between aryl and perfluoroaryl units lead to the formation of the corrugated layers.

The crystal structure of the **1·pfp**₃ complex (the triclinic space group $P\bar{1}$) reveals a layered structure. The layers, however, parallel to the (2−11) family of planes, are strongly corrugated due to the nonplanarity of the component units (Figure 2a). Two phenyl rings of **1** are twisted by about 31 and 32° from the plane of the central aryl ring, whereas the third one remains almost coplanar with it. In contrast, in the uncomplexed

molecule all three phenyl rings are twisted by ca. 36−41° from the central ring.[64] This arrangement is closely mimicked by the **pfp**₃ trimer. One $C_6F_5$ ring is nearly coplanar with the plane established by the three oxygen atoms and the other two remain out of the plane by 17.3(3) and 31.9(2)° (Table S2). The component units within the layers are held together by numerous weak C−H···F interactions ($d_{C−H···F}$ = 2.57−2.66 Å, Table S3). The alternating molecules of **1** and the **pfp**₃ trimers form infinite stacks, in direction of the *a* axis, with the phenyl and perfluorophenyl rings arranged in a parallel offset manner (Figure 2b). The distance between them is within the range of 3.34−3.47 Å.

The **2·pfp**₃ complex crystallizes in the monoclinic $P2/n$ space group, and the asymmetric unit is constituted by one half of the molecule **2** and one and half of **pfp**. Both **2** and the trimer obey twofold rotation molecular symmetry. The hydrogen atoms in hydroxyl groups are disordered over two positions with a site occupation factor of 0.5 (Figure 3a). The molecule of **2** in the cocrystal is slightly less twisted than the uncomplexed one. The corresponding dihedral angles are 29.30(6) and 37.40(6)°, whereas those in the free compound are 35.15(7), 39.95(8), and 42.93(6)°.[65] The geometry of the **pfp**₃ trimer, lying on the twofold rotation axis, follows restrains of the point group 2 (Schoenflies $C_2$), so determined electron density reflects the mean value of two molecules which differ in orientation of the hydrogen bonding loop, so all OH hydrogen atoms are occupied in 1/2 at the two positions. As in the previous example, the complex **2·pfp**₃ shows a layered structure, with the layers parallel to (10−1) family of planes, stabilized by the C(sp³)−H···F interactions and the F···F contacts. This structure is unique because the alternating layers are composed of only one type of molecules (Figure 3b) and additionally each layer has its own

symmetry having twofold rotation axes, inversion centers in plane, and perpendicular glide planes giving together the subperiodic layer group $p2/b11$ (L16 in IUCr Tables Vol. E)[66] (Table S4). The group symbol refers to the subperiodic setting ($b$, $a − c$, $a + c$). The almost parallel 4-methylphenyl and pentafluorophenyl units form infinite alternating stacks in the direction of the crystallographic $a$ axis.

To obtain cocrystals with flat **pfp**$_3$ trimers, we decided to utilize molecules able to adopt planar conformation. First, we tested 1,3,5-tripyrrolylbenzene[49] but cocrystallization attempts yielded only crystals of the uncomplexed compound. The most probable reason being that the size of the coformer molecules does not match the size of the trimer. Therefore, there was a need to enlarge the substituents at the central benzene ring of the star-shaped compound without losing its flatness. We chose 1,3,5-tris(5-methylthiophen-2-yl)benzene (**3**) bearing a methyl group on the substituent making it a bit larger than the pyrrolyl derivative. First attempts were unsuccessful and crystals of pure **3** were obtained. However, after using a large excess of **pfp** during cocrystallization, we were able to obtain the desired cocrystal with the right stoichiometry. During further investigation, we replaced the central benzene ring with boroxine and 1,3,5-triazine rings. In that way, we could introduce flat phenyl derivatives to our series (compounds **4** and **5**). These coformers easily afforded cocrystals containing the **pfp**$_3$ trimers. Next, we checked 1,3,5-tris(phenylethynyl)benzene (**6**) where phenyl rings are separated by C≡C bonds, which also enables the molecules to adopt planar conformation. To our delight, we obtained cocrystals with an excellent fit of the molecules of **6** and the **pfp**$_3$ trimers. Moreover, the crystal structure belongs to a trigonal space group which is rarely observed in organic crystals.

In cocrystals **3·pfp**$_3$−**6·pfp**$_3$, the essentially planar trimers **pfp**$_3$ are additionally stabilized by two or three F···F interactions between perfluorophenyl rings within the trimer and between them.[67,68] Parameters for the interactions are $d_{F···F}$ = 2.70−2.93 Å and $\theta_{C−F···F}$ = 143−149° (see Table 2). The cocrystals revealed layered structures composed of flat or slightly corrugated sheets containing nearly planar **pfp**$_3$ trimers and the triaryl molecules. Due to a matching shape of the component molecules the layers are stabilized by weak C−H···F interactions

between aryl and perfluoroaryl units ($d_{C−H···F}$ = 2.44−2.67 Å and $\theta_{C−H···F}$ = 123−171°, Table S3). It has been evidenced by Desiraju and coworkers that the C−H···F interactions are structurally similar to the C−H···O or C−H···N interactions and make a significant contribution to crystal packing and its stabilization.[69] The interlayer association occurs through $\pi···\pi$ interaction between aryl and perfluoroaryl rings which form offset face-to-face alternating stacks.

The complex **3·pfp**$_3$ crystallizes in the triclinic space group $P\bar{1}$ and the asymmetric unit contains one molecule of **3** and three **pfp** units forming a hydrogen-bonded $R_3^3(6)$ motif (Figure 4a). Determination of its crystal structure revealed layers, parallel to (20−2) family of planes, composed of nearly planar **pfp**$_3$ trimers and slightly distorted from planarity molecules of **3** (the dihedral angles between the mean planes of the central benzene and the thienyl rings are ca. 9°). The geometry of **3** deviates from the threefold symmetry because one of the three 5-methylthienyl moieties (with S1 atom) is rotated by 180° around the C19−C34 bond, making unsymmetrical conformation. This kind of orientation is also found in the uncomplexed molecule (see the Supporting Information). The conformation in the cocrystal enhances the number of short $C_{Ar}$−H···F contacts within the layers. The alternating units **3** and **pfp**$_3$ are arranged side-to-side into parallel and nearly flat rows stabilized by weak $C_{Ar}$−H···F and $C(sp^3)$−H···F interactions (see Table S3). The rows are further assembled into slightly corrugated layers in the form of low staircase (Figure 4b). The **pfp** molecules in the nearly planar **pfp**$_3$ trimers are held together by the cyclic motif **III**. For parameters, see Table 1. Two short F···F contacts are present within the trimer (Table 2) which are 8% shorter than the sum of van der Waals radii of the two F atoms. The alternating **pfp**$_3$ trimers and the molecules of **3** form infinite offset stacks stabilized by $\pi···\pi$ interactions between aryl and perfluoroaryl units. The distance between the $\pi···\pi$ planes are in the range of 3.35−3.53 Å and the centroids of the thienyl and pentafluorophenyl rings in the stack are in the range of 3.56−3.79 Å and the dihedral angle between planes formed by aryl and perfluoroaryl rings does not exceed 7°.

The boroxine complex **4·pfp**$_3$ also crystallizes in the $P\bar{1}$ space group and its crystal structure resembles that of the described above. It is composed of stacked flat layers, parallel to (202) family of planes, where the alternating **pfp**$_3$ trimers and the molecules of **4** are arranged in parallel rows running along the $a$ axis (Figure 5). The molecules within the layer are held together by weak C−H···F interactions between **4** and **pfp**$_3$ (an average H···F distance is 2.65 Å being only 1% shorter than the sum of their van der Waals radii) and F···F contacts (2.81−2.86 Å) between the **pfp**$_3$ units. The molecules of **4** assume nearly planar conformation with the phenyl rings inclined by 4.6, 5.8, and 10.8° to the central boroxine ring which resembles the geometry of the uncomplexed compound.[70] The nearly planar trimers are stabilized by HBs with an average distance and valence angle of 2.11 Å and 135°, respectively (Table 1). Three F···F contacts are present within the trimer (Table 2) about 2, 4, and 7% shorter than the sum of van der Waals radii of the two atoms. The aryl··· perfluoroaryl stacking interactions between alternating **4** and **pfp**$_3$ units result in the formation of infinite slipped stacks (Figure 5b). Distances between centroids of the aryl and perfluoroaryl rings are within the range of 3.69−3.98 Å with the stack slip angle of about 27°.

The crystal structure of the **5·pfp**$_3$ complex (the triclinic $P\bar{1}$ space group) closely resembles those of two previous complexes (Figure 6). The alternating **5** and **pfp**$_3$ units are organized in
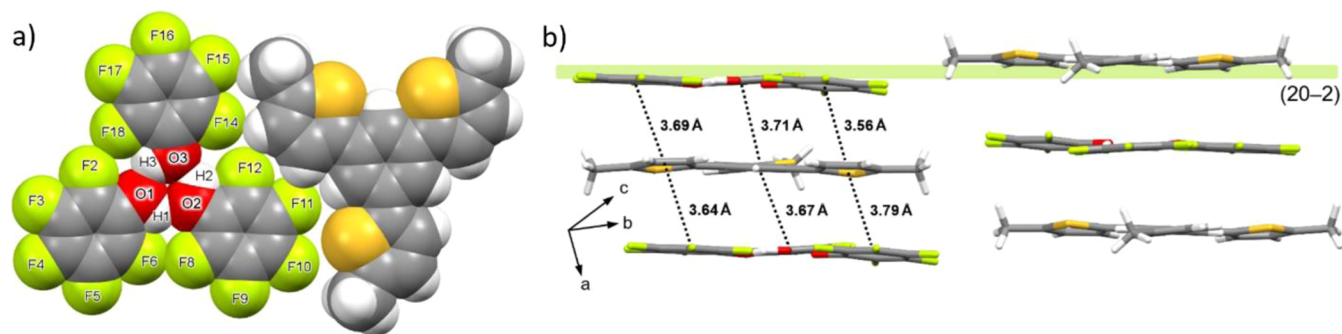
**Table 2. Parameters of the F···F Contacts within the pfp**$_3$ **Trimer**[a]

| cocrystal | interaction | $d_{F···F}$ (Å) | $\theta_{C−F···F}$ (deg)[b] | $\delta_\%$ (%) |
|---|---|---|---|---|
| **3·pfp**$_3$ | F2···F18 | 2.699(5) | 142.5(4) | 92 |
| | F6···F8 | 2.713(6) | 144.3(4) | 92 |
| **4·pfp**$_3$ | F2···F14 | 2.829(3) | 146.2(3) | 96 |
| | F6···F8 | 2.747(3) | 148.8(3) | 93 |
| | F12···F18 | 2.877(4) | 147.0(3) | 98 |
| **5·pfp**$_3$ | F2···F18 | 2.862(12) | 146.1(8) | 97 |
| | F6···F8 | 2.934(12) | 147.6(8) | 99.8 |
| | F12···F14 | 2.765(12) | 148.0(9) | 94 |
| **6·pfp**$_3$ | F2···F18 | 2.791(5) | 144.6(3) | 95 |
| | F6···F8 | 2.791(4) | 146.9(3) | 95 |
| | F12···F14 | 2.828(4) | 145.6(3) | 96 |
| | F20···F36 | 2.783(4) | 148.1(3) | 95 |
| | F24···F26 | 2.798(5) | 147.6(3) | 95 |
| | F30···F32 | 2.802(3) | 145.3(3) | 95 |

[a]The parameter $\delta_\%$ corresponds to the ratio of the $d_{F···F}$ and the sum of van der Waals radii of the two atoms. [b]The smaller value is reported.

**Figure 4.** Crystal structure of **3·pfp₃**: (a) view of the **pfp₃** trimer and the molecule of **3** with numbering of the OH groups and F atoms; (b) projection along the layers with Miller index of a family of parallel planes with the same orientation together with distances between centroids of the interacting rings (dotted lines).



**Figure 5.** Crystal structure of **4·pfp₃**: (a) view of the **pfp₃** trimer and the molecule of **4** with numbering of the OH groups and F atoms; (b) projection along the layers with Miller index of a family of parallel planes with the same orientation together with distances between centroids of the interacting rings (dotted lines).
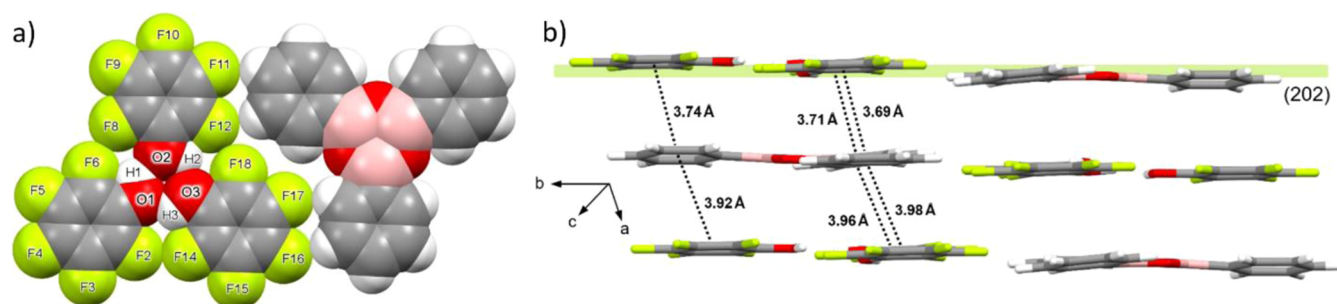


**Figure 6.** Crystal structure of **5·pfp₃**: (a) view of the **pfp₃** trimer and the molecule of **5** with numbering of the OH groups and F atoms; (b) projection along the layers with Miller index of a family of parallel planes with the same orientation together with distances between centroids of the interacting rings (dotted lines).
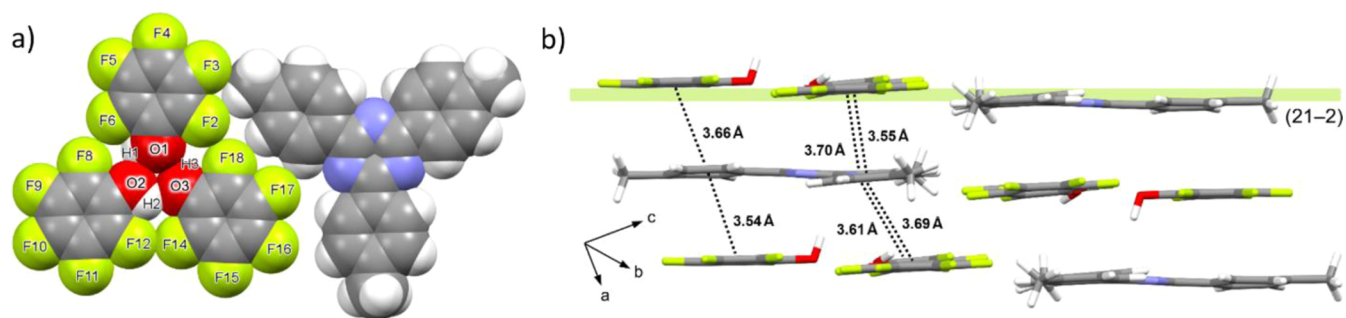
stacks running along the *a* axis and forming nearly planar sheets, parallel to (21−2) family of planes, with the component units held together by the C−H⋯F interactions (Table S3). The triazine molecule **5** is only slightly distorted from planarity (the dihedral angles between the mean planes of the central triazine and the *p*-tolyl rings do not exceed 9°) and its geometry closely corresponds to that of the uncomplexed molecule.[71] The nearly planar trimers are stabilized by three HBs and three F⋯F interactions (Tables 1 and 2). The **5** and **pfp₃** units are arranged into π⋯π stacked columns—the distances between centroids of aryl and perfluoroaryl rings are in the range of 3.54−3.70 Å with a slip angle of about 21° (Figure 6b). There are no strong, linear O−H⋯N HBs between the central triazine unit and the **pfp** molecules, indicating that the formation of the **pfp₃** trimer is preferable to these interactions. However, one hydrogen atom of the **pfp₃** trimer points toward the π-basic central triazine ring (the distance between H3 and the centroid of the triazine ring is

2.35 Å, and the distance to the nearest nitrogen atom is $d_{H3⋯N1}$ = 2.59 Å).

The complex **6·pfp₃** crystallizes in the space group $P3_2$ and the asymmetric unit contains two molecules of **6** and six of **pfp** arranged into **pfp₃** trimers (Figure 7a). It shows an unusual and aesthetically pleasing layered structure due to the excellent fit of the component molecules within the layer, parallel to the (006) family of planes (Figure 7b). The molecules of **6** assume nearly coplanar conformation (the corresponding dihedral angles are in the range of 1.0−10.7°) that contrasts with the strongly twisted geometry of the molecules in the crystals of pure **6**.[55] Each molecule of **6** is surrounded by three essentially coplanar **pfp₃** trimers connected with them via numerous C−H⋯F contacts (often bifurcated) forming flat sheets. The shortest C−H⋯F bonds are 7% shorter than the sum of van der Waals radii of the H and F atoms (the average $d_{C−H⋯F}$ is 2.61 Å, Table S3). The π⋯π stacking interaction between the layers is more complex
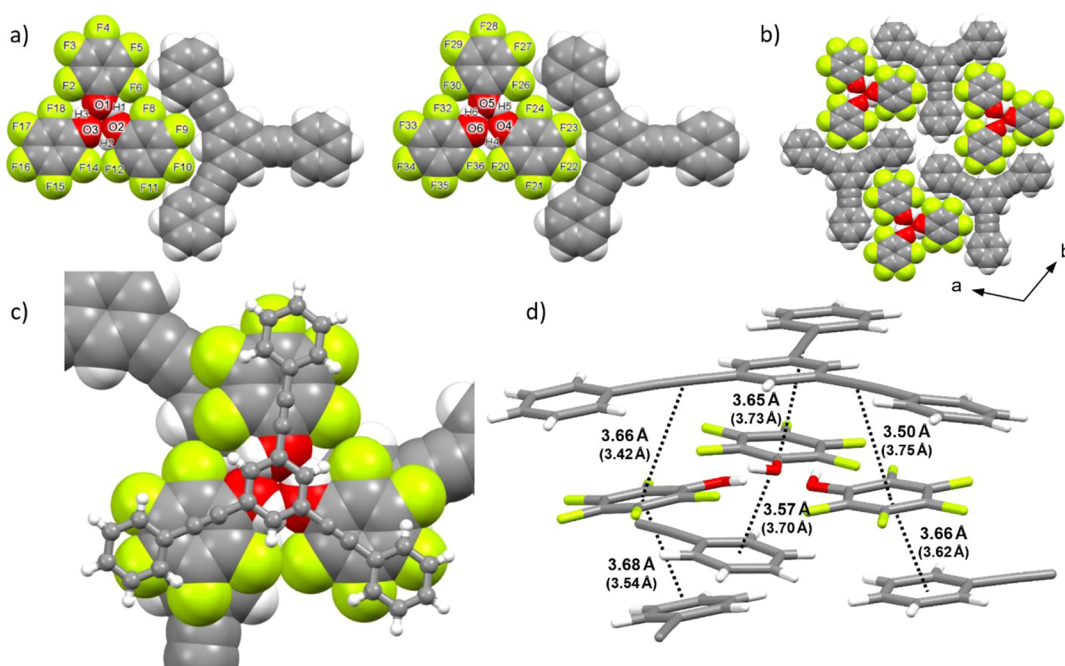
**Figure 7.** Crystal structure of **6·pfp$_3$**: (a) view of the **pfp$_3$** trimers and molecules of **6** with numbering of the OH groups and F atoms; (b) fragment of one layer of molecules; (c) $\pi\cdots\pi$ stacking interactions between **pfp$_3$** trimer and molecules of **6**; and (d) view of the interactions with distances between centroids of the interacting rings and centroids of the triple bonds (dotted lines), in parentheses values for the second symmetry-independent **pfp$_3$** trimer are given.
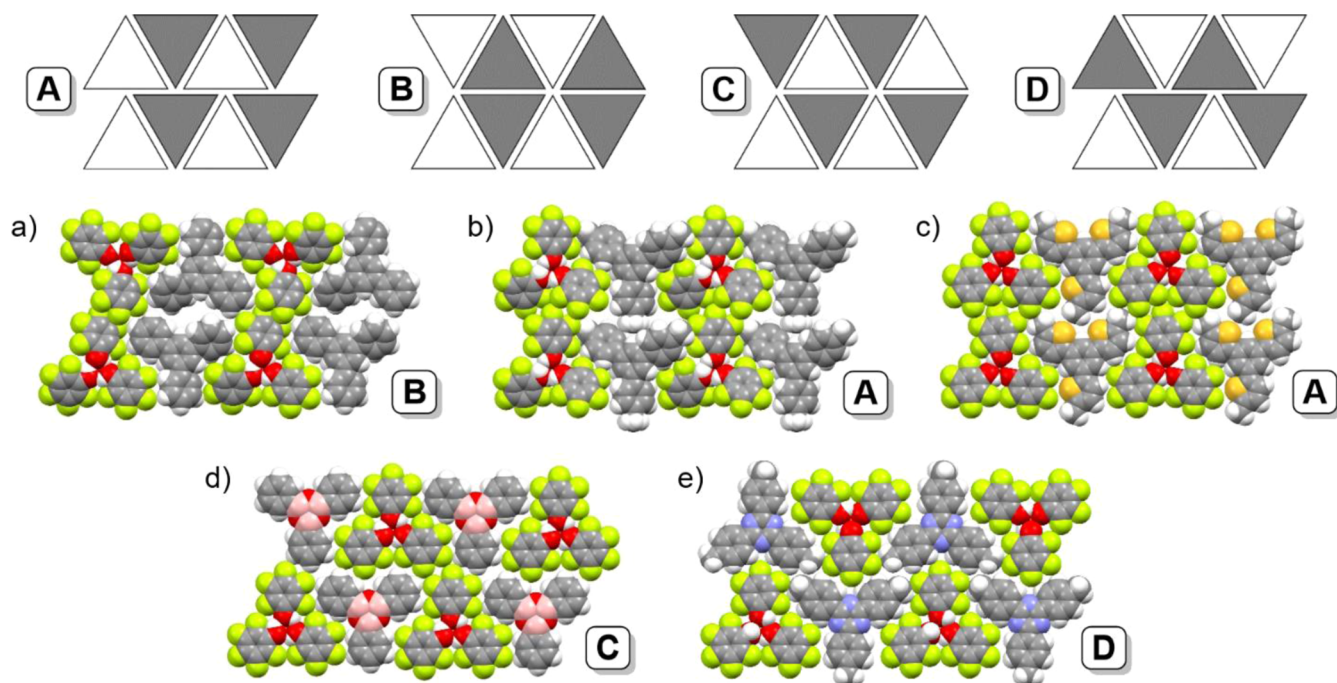


**Figure 8.** Structural motifs **A−D** found within one layer in cocrystals of (a) **1·pfp$_3$**; (b) **2·pfp$_3$**; (c) **3·pfp$_3$**; (d) **4·pfp$_3$**; and (e) **5·pfp$_3$**. In the case of **2·pfp$_3$**, the molecules were selected in such a way to show the mutual orientation of the molecules (view along the *a* axis).

than in previous examples. It involves not only aryl rings but also ethynyl moieties, both being $\pi$-basic (see Figure 1). Each pentafluorophenyl ring is located between parallel phenyl and ethynyl units (Figure 7c,d). The average distance between the centroid of the C$_6$F$_5$ ring and the center of the triple bond is 3.62 Å, whereas the distance between centroids of the phenyl and perfluorophenyl rings is in the range of 3.54−3.70 Å.

In the cocrystals of **1−5** four different structural motifs **A−D** were identified within a single layer. They are schematically represented in Figure 8, where each **pfp$_3$** trimer is marked with a white and the coformer molecule with a gray triangle. In motif **A**, each horizontal row of molecules is duplicated in both directions in the same orientation, and in **B**, every second row is inverted. Consequently, the trimers are arranged in vertical columns separated by similar columns of the triaryl molecules. This
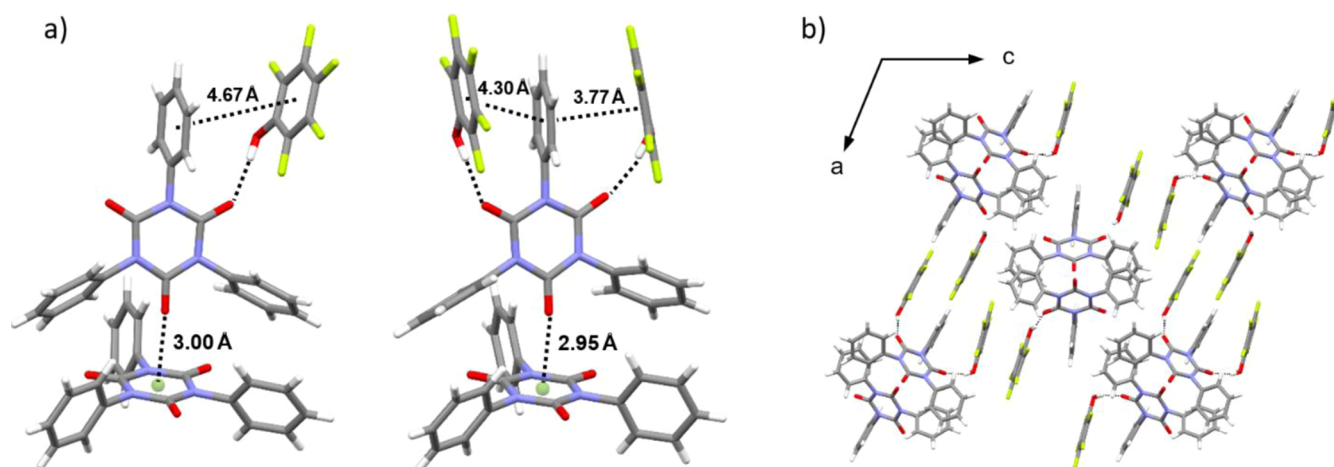
**Figure 9.** Crystal structure of **7·pfp**: (a) view of the HBs, $\pi\cdots\pi$ and anion$\cdots\pi$-like interactions in the stacks of both symmetry-independent molecules of 7; (b) projection along the *b* axis.
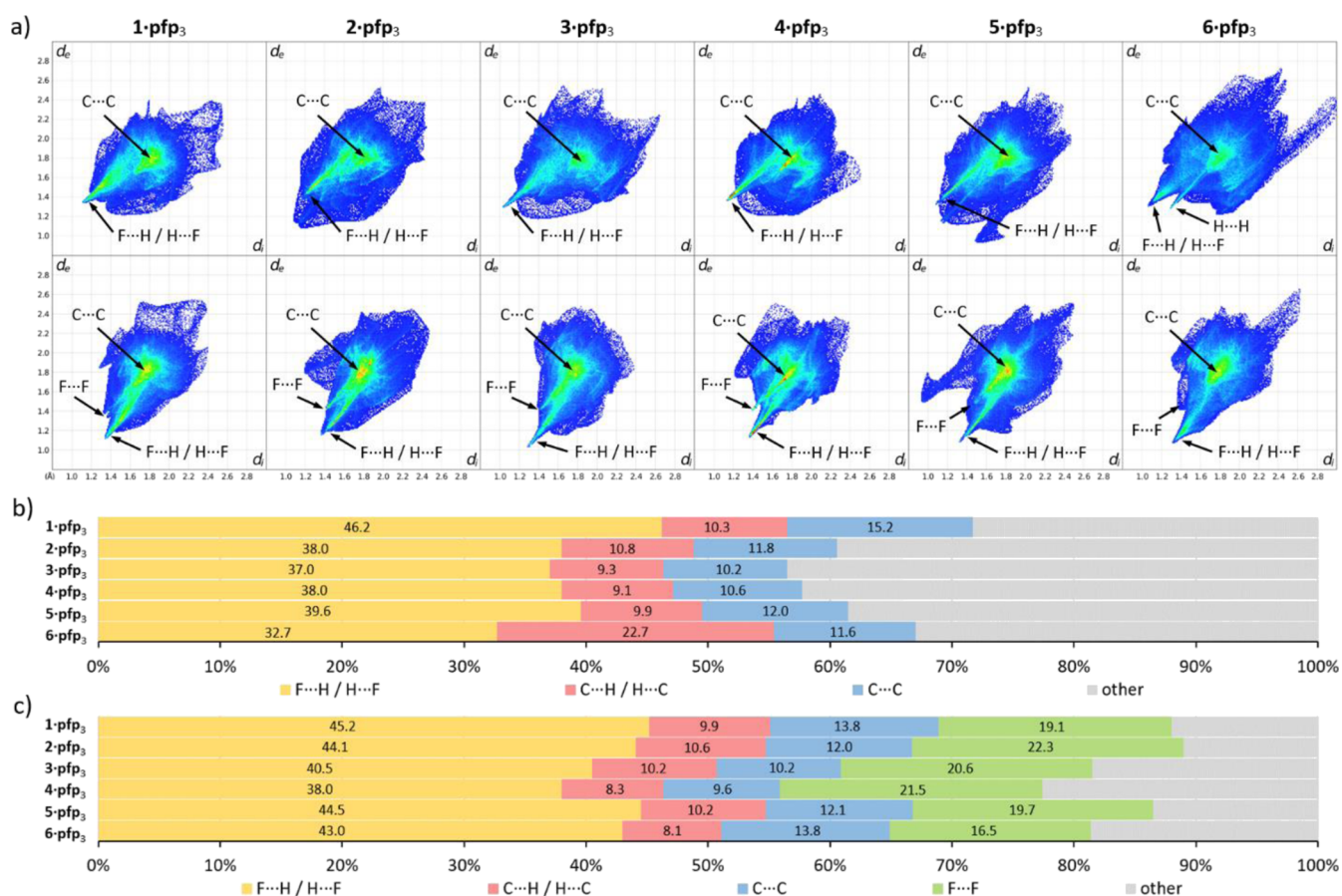


**Figure 10.** Two-dimensional fingerprint plots of **1–6** [(a) top] and the **pfp₃** trimers [(a) bottom] in the cocrystals **1·pfp₃–6·pfp₃**. Selected intermolecular contacts are highlighted. The percentage contributions of selected close intermolecular contacts to the HS area based on the coformer molecule (b) and the **pfp₃** trimer (c). Other contacts are highlighted in gray; all values on the diagram are expressed in %.

creates the possibility to form F$\cdots$F contacts between **pfp₃** trimers. Indeed, these interactions do occur in cocrystals **1·pfp₃**, **2·pfp₃**, and **3·pfp₃**. In arrangement **C**, every second row is translated and in **D**, both translated and inverted. In these motifs the trimers are further apart, and in the case of **5·pfp₃** (motif D), such contacts within one layer are not observed.

In contrast to the previous star-shaped compounds tested, triphenyl isocyanurate (**7**), in which all phenyl rings are almost perpendicular to the central heterocyclic ring, with **pfp** forms a

2:3 complex with no trimers **III**. The asymmetric unit of the complex (the space group $P2_1$) consists of two symmetry-independent strongly twisted molecules of **7** and three **pfp** units. The conformation of **7** closely resembles that of the uncomplexed molecule.[72] This kind of molecular geometry obviously precludes the formation of the layered 2D structure but some $\pi\cdots\pi$ stacking interactions are still possible. The **pfp** molecules, instead of forming trimers, interact with **7** by O–H$\cdots$O=C HBs (Table 1). One molecule of **7** binds to two **pfp** units

in such a way that a phenyl ring is located between two pentafluorophenyl moieties, and the other interacts with only one **pfp** (Figure 9a). The molecules of **7** themselves are arranged in columns running along the $b$ axis (Figure 9b), where the carbonyl oxygen atoms are in proximity to the $\pi$-acidic isocyanurate rings resembling anion$\cdots\pi$ interactions. This arrangement is also observed in one of the polymorphs (orthorhombic $Fdd2$ space group) of the pure compound **7**.[72]

**HS Analysis.** To assess the percent distribution of some contacts present in the crystal structures of $\mathbf{1 \cdot pfp_3}$–$\mathbf{6 \cdot pfp_3}$, HS analysis was performed. In each case, HS of both the $\mathbf{pfp_3}$ trimer and its coformer was calculated and a fingerprint plot was generated. Results are presented in Figure 10.

The plots for coformer molecules exhibit one main spike corresponding to the H$\cdots$F/F$\cdots$H contacts. Its minimum $d_e + d_i$ value is in the range of 2.3–2.6 Å being shorter than the sum of the van der Waals radii of H and F atoms (2.67 Å). The fingerprint plot of **6** contains additional spike representing H$\cdots$H contacts. The plots for $\mathbf{pfp_3}$ trimers contain two sharp spikes, indicating the H$\cdots$F/F$\cdots$H and F$\cdots$F interactions. The average minimum $d_e + d_i$ value for the inter-halogen interactions is at about 2.8 Å ($\delta_\% \approx 95\%$). In the middle of each graph (both for coformer and $\mathbf{pfp_3}$ trimer), there is a region denoting the C$\cdots$C contacts.

The fingerprint plots for the $\mathbf{pfp_3}$ trimers and their coformers **1**–**6** look quite different in most cases. How similar the percentage distributions are can be seen when they are presented in the form of a diagram (Figure 10b,c). The degree of sameness is understandable as most contacts are reciprocal for both components.

Intermolecular H$\cdots$F interactions have the highest contribution in all of the cocrystals studied (33–46%) which can be rationalized by the proximity of these atoms within the layers and between them. For $\mathbf{1 \cdot pfp_3}$, the H$\cdots$F contacts constitute as much as 46.2% (based on **1**) and 45.2% (based on $\mathbf{pfp_3}$) of the HS which can be attributed to the fact that the layers are significantly corrugated. The contribution of these interactions for $\mathbf{2 \cdot pfp_3}$ is also relatively high (38.0 and 44.1%) despite the presence of the separate layers of the $\mathbf{pfp_3}$ trimers and molecules of **2**. Surprisingly, for $\mathbf{6 \cdot pfp_3}$, where there is such a perfect fit of the molecules, the lowest value of the H$\cdots$F interactions based on **6** is observed (32.7%). However, this may be due to the size of the coformer molecule compared to the other ones. In almost every case, the C$\cdots$H contacts account for about 10% of the HS. The cocrystal which stands out is again $\mathbf{6 \cdot pfp_3}$ (22.7%). This fact can be explained by the proximity of three phenyl rings of three **6** molecules to the $\mathbf{pfp_3}$ trimer. The C$\cdots$C contacts reflecting mostly the $\pi\cdots\pi$ interactions of aryl and perfluoroaryl rings for each cocrystal are in the range of 10–15%. HSs of the $\mathbf{pfp_3}$ trimers revealed that the F$\cdots$F contacts account for 17–22% of the total number of interactions. The largest value of 22.3% belongs to $\mathbf{2 \cdot pfp_3}$, which again is associated with the fact that in this cocrystal, the components' molecules form separate layers.

To better visualize the $\pi\cdots\pi$ stacking interactions, HSs mapped on the shape index and curvedness were generated and analyzed. The surfaces for $\mathbf{1 \cdot pfp_3}$ are presented in Figure 11.

On the shape index maps generated in the range of −1 to 1 Å for each cocrystal, there are adjacent red and blue triangles characteristic for the $\pi\cdots\pi$ stacking interactions[73,74] (yellow dashed ellipses in Figure 11). The blue convex triangle corresponds to a carbon atom of an aryl ring within the considered surface and the red concave triangle represents a carbon atom of an aromatic ring outside the surface. The
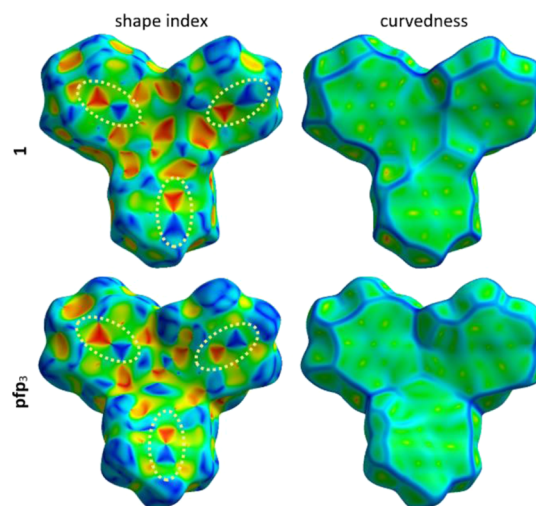


**Figure 11.** HSs of **1** and $\mathbf{pfp_3}$ in $\mathbf{1 \cdot pfp_3}$ mapped with $d_{norm}$, shape index, and curvedness. Areas of $\pi\cdots\pi$ stacking interactions are highlighted as yellow dashed ellipses.

curvedness maps (generated from −4 to 0.4 Å) of both components show large flat green areas corresponding to the phenyl and perfluorophenyl rings, which also indicates clearly $\pi\cdots\pi$ interactions.

It should be mentioned that both sides of the shape index and curvedness surfaces look quite similar because the components are arranged into infinite stacks. The exception is $\mathbf{6 \cdot pfp_3}$, where **6** interacts with the whole $\mathbf{pfp_3}$ trimer on one side and three phenyl rings with three **pfp** molecules of three different $\mathbf{pfp_3}$ trimers on the other (see Figures S7 and S8).

HSs of both components of $\mathbf{1 \cdot pfp_3}$–$\mathbf{6 \cdot pfp_3}$ mapped with $d_{norm}$, shape index, and curvedness are presented in the Supporting Information.

All the results presented above clearly demonstrate that the weak perfluoroaryl$\cdots$aryl stacking interactions are valuable tools in controlling the arrangement of aromatic units in crystal engineering and bring out the relevance of weak noncovalent interactions where organic fluorine atom $C(sp^2)$–F is involved. One can also notice that it is the weak C–H$\cdots$F and F$\cdots$F forces directing the packing into relevant planes to generate unique packing motifs. On the other hand, while the uncomplexed molecules **1**–**6** possess more twisted geometry, the $\pi\cdots\pi$ interactions force these molecules in cocrystals to adopt more planar conformation.

## ■ CONCLUSIONS

To conclude, we thoroughly investigated the $\pi\cdots\pi$ stacking interactions between aryl and perfluoroaryl moieties in the molecular crystals of **pfp** with star-shaped triaryl derivatives. The aggregation of the **pfp** molecules into hydrogen-bonded cyclic trimers with the central $R_3^3(6)$ motif (**III**) can be supported and enhanced by the $\pi\cdots\pi$ stacking interactions. Furthermore, the layered structure of the cocrystals is stabilized by numerous weak intermolecular C–H$\cdots$F and F$\cdots$F interactions. The results strongly suggest that in order to form cocrystals with the desired trimers, the triaryl component must have the size and shape comparable with that of $\mathbf{pfp_3}$ and, ideally, it should be able to adopt a planar conformation. However, some degree of tolerance is acceptable because the trimers are flexible and stable enough to mimic the shape of the coformer, as in $\mathbf{1 \cdot pfp_3}$ and $\mathbf{2 \cdot pfp_3}$. Additionally, there is a question whether the star-

shaped component may contain any additional functional groups able to compete with **pfp** in forming HBs. However, despite the fact that molecules of **4** and **5** contain oxygen and nitrogen atoms, respectively, being relatively strong HB acceptors, no additional HBs with these atoms are formed and the aryl···perfluoroaryl interactions induce the formation of motif **III**. Finally, strongly deviated from planarity triaryl component **7** is not able to induce the formation of the **pfp**$_3$ trimers and the structure of its **pfp** cocrystal is mainly controlled by intermolecular O−H···O=C HBs.

## ■ ASSOCIATED CONTENT

### ⓈⒾ Supporting Information

The Supporting Information is available free of charge at https://pubs.acs.org/doi/10.1021/acs.cgd.2c00276.

> Details on X-ray crystallography, description of the crystal structure of **3**, HSs, and percentage contributions of all contacts to the HSs (PDF)

### Accession Codes

CCDC 2145256−2145262 contain the supplementary crystallographic data for this paper. These data can be obtained free of charge via www.ccdc.cam.ac.uk/data_request/cif, or by emailing data_request@ccdc.cam.ac.uk, or by contacting The Cambridge Crystallographic Data Centre, 12 Union Road, Cambridge CB2 1EZ, UK; fax: +44 1223 336033.

## ■ AUTHOR INFORMATION

### Corresponding Author

**Teresa Olszewska** − *Department of Organic Chemistry, Faculty of Chemistry, Gdańsk University of Technology, 80-233 Gdańsk, Poland;* ⓞ orcid.org/0000-0003-1477-1562; Phone: +48 58 347 14 25; Email: teresa.olszewska@pg.edu.pl

### Authors

**Jan Alfuth** − *Department of Organic Chemistry, Faculty of Chemistry, Gdańsk University of Technology, 80-233 Gdańsk, Poland;* ⓞ orcid.org/0000-0003-3428-5705

**Jarosław Chojnacki** − *Department of Inorganic Chemistry, Faculty of Chemistry, Gdańsk University of Technology, 80-233 Gdańsk, Poland*

**Tadeusz Połoński** − *Department of Organic Chemistry, Faculty of Chemistry, Gdańsk University of Technology, 80-233 Gdańsk, Poland;* ⓞ orcid.org/0000-0003-2994-7954

**Aleksander Herman** − *Department of Inorganic Chemistry, Faculty of Chemistry, Gdańsk University of Technology, 80-233 Gdańsk, Poland*

**Maria J. Milewska** − *Department of Organic Chemistry, Faculty of Chemistry, Gdańsk University of Technology, 80-233 Gdańsk, Poland;* ⓞ orcid.org/0000-0002-9740-0881

Complete contact information is available at:
https://pubs.acs.org/10.1021/acs.cgd.2c00276

### Author Contributions

The manuscript was written through contributions of all authors. All authors have given approval to the final version of the manuscript.

### Notes

The authors declare no competing financial interest.

## ■ REFERENCES

(1) Hunter, C. A. The Role of Aromatic Interactions in Molecular Recognition. *Chem. Soc. Rev.* **1994**, *23*, 101−109.

(2) Hunter, C. A.; Lawson, K. R.; Perkins, J.; Urch, C. J. Aromatic Interactions. *J. Chem. Soc., Perkin Trans.* **2001**, *2*, 651−669.

(3) Janiak, C. Critical Account on $\pi$-$\pi$ Stacking in Metal Complexes with Aromatic Nitrogen-Containing Ligands. *J. Chem. Soc., Dalton Trans.* **2000**, 3885−3896.

(4) Thakuria, R.; Nath, N. K.; Saha, B. K. The Nature and Applications of $\pi$-$\pi$ Interactions: A Perspective. *Cryst. Growth Des.* **2019**, *19*, 523−528.

(5) Martinez, C. R.; Iverson, B. L. Rethinking the Term "Pi-Stacking". *Chem. Sci.* **2012**, *3*, 2191−2201.

(6) Hwang, J. w.; Li, P.; Shimizu, K. D. Synergy between Experimental and Computational Studies of Aromatic Stacking Interactions. *Org. Biomol. Chem.* **2017**, *15*, 1554−1564.

(7) Saenger, W. *Principles of Nucleic Acid Structure*; Springer-Verlag: New York, 1984.

(8) Li, S.; Cooper, V. R.; Thonhauser, T.; Lundqvist, B. I.; Langreth, D. C. Stacking Interactions and DNA Intercalation. *J. Phys. Chem. B* **2009**, *113*, 11166−11172.

(9) Mcgaughey, G. B.; Gagné, M.; Rappé, A. K. $\pi$-Stacking Interactions Alive and Well in Proteins. *J. Biol. Chem.* **1998**, *273*, 15458−15463.

(10) Klosterman, J. K.; Yamauchi, Y.; Fujita, M. Engineering Discrete Stacks of Aromatic Molecules. *Chem. Soc. Rev.* **2009**, *38*, 1714−1725.

(11) Sergeyev, S.; Pisula, W.; Geerts, Y. H. Discotic Liquid Crystals: A New Generation of Organic Semiconductors. *Chem. Soc. Rev.* **2007**, *36*, 1902−1929.

(12) Shoseyov, O.; Levy, I. *Nanobiotechnology: BioInspired Devices and Materials of the Future*; Humana Press, 2008.

(13) Jorgensen, W. L.; Severance, D. L. Aromatic-Aromatic Interactions: Free Energy Profiles for the Benzene Dimer in Water, Chloroform, and Liquid Benzene. *J. Am. Chem. Soc.* **1990**, *112*, 4768−4774.

(14) Sinnokrot, M. O.; Valeev, E. F.; Sherrill, C. D. Estimates of the Ab Initio Limit for $\pi$-$\pi$ Interactions: The Benzene Dimer. *J. Am. Chem. Soc.* **2002**, *124*, 10887−10893.

(15) Lorenzo, S.; Lewis, G. R.; Dance, I. Supramolecular Potentials and Embraces for Fluorous Aromatic Molecules. *New J. Chem.* **2000**, *24*, 295−304.

(16) Hernández-Trujillo, J.; Colmenares, F.; Cuevas, G.; Costas, M. MP2 Ab Initio Calculations of the Hexafluorobenzene-Benzene and -Monofluorobenzene Complexes. *Chem. Phys. Lett.* **1997**, *265*, 503−507.

(17) Williams, J. H. The Molecular Electric Quadrupole Moment and Solid-State Architecture. *Acc. Chem. Res.* **1993**, *26*, 593−598.

(18) Hernández-Trujillo, J.; Costas, M.; Vela, A. Quadrupole Interactions in Pure Non-Dipolar Fluorinated or Methylated Benzenes and Their Binary Mixtures. *J. Chem. Soc., Faraday Trans.* **1993**, *89*, 2441−2443.

(19) Patrick, C. R.; Prosser, G. S. A Molecular Complex of Benzene and Hexafluorobenzene. *Nature* **1960**, *187*, 1021.

(20) Gavezzotti, A. On the Preferred Mutual Orientation of Aromatic Groups in Organic Condensed Media. *Chem. Phys. Lett.* **1989**, *161*, 67−72.

(21) Reichenbächer, K.; Süss, H. I.; Hulliger, J. Fluorine in Crystal Engineering—"the Little Atom That Could". *Chem. Soc. Rev.* **2005**, *34*, 22−30.

(22) Bacchi, S.; Benaglia, M.; Cozzi, F.; Demartin, F.; Filippini, G.; Gavezzotti, A. X-Ray Diffraction and Theoretical Studies for the Quantitative Assessment of Intermolecular Arene-Perfluoroarene Stacking Interactions. *Chem.—Eur. J.* **2006**, *12*, 3538–3546.

(23) Hashim, M. I.; Le, H. T. M.; Chen, T.-H.; Chen, Y.-S.; Daugulis, O.; Hsu, C.-W.; Jacobson, A. J.; Kaveevivitchai, W.; Liang, X.; Makarenko, T.; Miljanić, O. Š.; Popovs, I.; Tran, H. V.; Wang, X.; Wu, C.-H.; Wu, J. I. Dissecting Porosity in Molecular Crystals: Influence of Geometry, Hydrogen Bonding, and [$\pi\cdots\pi$] Stacking on the Solid-State Packing of Fluorinated Aromatics. *J. Am. Chem. Soc.* **2018**, *140*, 6014–6026.

(24) Smith, C. E.; Smith, P. S.; Thomas, R. L.; Robins, E. G.; Collings, J. C.; Dai, C.; Scott, A. J.; Borwick, S.; Batsanov, A. S.; Watt, S. W.; Clark, S. J.; Viney, C.; Howard, J. A. K.; Clegg, W.; Marder, T. B. Arene-Perfluoroarene Interactions in Crystal Engineering: Structural Preferences in Polyfluorinated Tolans. *J. Mater. Chem.* **2004**, *14*, 413–420.

(25) Collings, J. C.; Roscoe, K. P.; Robins, E. G.; Batsanov, A. S.; Stimson, L. M.; Howard, J. A. K.; Clark, S. J.; Marder, T. B. Arene-perfluoroarene interactions in crystal engineering. Part 3. Single-crystal structures of 1:1 complexes of octafluoronaphthalene with fused-ring polyaromatic hydrocarbons. *New J. Chem.* **2001**, *25*, 1410–1417.

(26) Cozzi, F.; Bacchi, S.; Filippini, G.; Pilati, T.; Gavezzotti, A. Synthesis X-Ray Diffraction and Computational Study of the Crystal Packing of Polycyclic Hydrocarbons Featuring Aromatic and Perfluoroaromatic Rings Condensed in the Same Molecule: 1,2,3,4-Tetrafluoronaphthalene, -Anthracene and -Phenanthrene. *Chem.—Eur. J.* **2007**, *13*, 7177–7184.

(27) Gdaniec, M.; Jankowski, W.; Milewska, M. J.; Połoñski, T. Supramolecular Assemblies of Hydrogen-Bonded Carboxylic Acid Dimers Mediated by Phenyl-Pentafluorophenyl Stacking Interactions. *Angew. Chem., Int. Ed.* **2003**, *42*, 3903–3906.

(28) Yamasaki, R.; Iida, M.; Ito, A.; Fukuda, K.; Tanatani, A.; Kagechika, H.; Masu, H.; Okamoto, I. Crystal Engineering of N,N′-Diphenylurea Compounds Featuring Phenyl-Perfluorophenyl Interaction. *Cryst. Growth Des.* **2017**, *17*, 5858–5866.

(29) Albrecht, M.; Yi, H.; Pan, F.; Valkonen, A.; Rissanen, K. Connecting Electron-Deficient and Electron-Rich Aromatics to Support Intermolecular Interactions in Crystals. *Eur. J. Org. Chem.* **2015**, 3235–3239.

(30) Cozzi, F.; Bacchi, S.; Filippini, G.; Pilati, T.; Gavezzotti, A. Competition between Hydrogen Bonding and Arene-Perfluoroarene Stacking. X-Ray Diffraction and Molecular Simulation on 5,6,7,8-Tetrafluoro-2-Naphthoic Acid and 5,6,7,8-Tetrafluoro-2-Naphthamide Crystals. *CrystEngComm* **2009**, *11*, 1122–1127.

(31) Althagbi, H. I.; Edwards, A. J.; Nicholson, B. K.; Reason, D. A.; Saunders, G. C.; Sim, S. A.; Van Der Heijden, D. A. Arene-Perfluoroarene-Anion Stacking and Hydrogen Bonding Interactions in Imidazolium Salts for the Crystal Engineering of Polarity. *Cryst. Growth Des.* **2016**, *16*, 174–188.

(32) Bhandary, S.; Chopra, D. Assessing the Significance of Hexafluorobenzene as a Unique Guest Agent through Stacking Interactions in Substituted Ethynylphenyl Benzamides. *Cryst. Growth Des.* **2018**, *18*, 3027–3036.

(33) Molčanov, K.; Milašinović, V.; Kojić-Prodić, B. Contribution of Different Crystal Packing Forces in $\pi$-Stacking: From Noncovalent to Covalent Multicentric Bonding. *Cryst. Growth Des.* **2019**, *19*, 5967–5980.

(34) Meejoo, S.; Kariuki, B. M.; Harris, K. D. M. The Interplay of Aryl-Perfluoroaryl Stacking Interactions and Interstack Hydrogen Bonding in Controlling the Structure of a Molecular Cocrystal. *ChemPhysChem* **2003**, *4*, 766–769.

(35) Piotrkowska, B.; Gdaniec, M.; Milewska, M. J.; Połoński, T. Aryl-Perfluoroaryl Stacking Interactions, Hydrogen Bonding and Steric Effects in Controlling the Structure of Supramolecular Assemblies of N,N′-Diaryloxalamides. *CrystEngComm* **2007**, *9*, 868–872.

(36) Eichstaedt, K.; Wasilewska, A.; Wicher, B.; Gdaniec, M.; Połoński, T. Supramolecular Synthesis Based on a Combination of Se⋯N Secondary Bonding Interactions with Hydrogen and Halogen Bonds. *Cryst. Growth Des.* **2016**, *16*, 1282–1293.

(37) Brock, C. P.; Duncan, L. L. Anomalous Space-Group Frequencies for Monoalcohols $C_nH_mOH$. *Chem. Mater.* **1994**, *6*, 1307–1312.

(38) Desiraju, G. R. The Supramolecular Synthons in Crystal Engineering - A New Organic Synthesis. *Angew. Chem., Int. Ed.* **1995**, *34*, 2311–2327.

(39) Munakata, M.; Wu, L. P.; Kuroda-sowa, T.; Maekawa, M.; Suenaga, Y.; Sugimoto, K.; Ino, I. Open dimeric and capped polymeric container molecules: calixarene and resorcinarene complexes of AgI co-ordinated by participation of the upper-rim carbon atoms. *J. Chem. Soc., Dalton Trans.* **1999**, 373–378.

(40) Mizyed, S.; Ashram, M.; Miller, D. O.; Georghiou, P. E. Supramolecular Complexation of [60]Fullerene with Hexahomotrioxacalix[3]Naphthalenes: A New Class of Naphthalene-Based Calixarenes. *J. Chem. Soc., Perkin Trans.* **2001**, 1916–1919.

(41) Sudbrake, C.; Müller, B.; Vahrenkamp, H. Hexakis(Alcohol)Zinc Complexes. *Eur. J. Inorg. Chem.* **1999**, *1999*, 2009–2012.

(42) Mukherjee, A.; Desiraju, G. R. Halogen Bonding and Structural Modularity in 2,3,4- and 3,4,5-Trichlorophenol. *Cryst. Growth Des.* **2011**, *11*, 3735–3739.

(43) Zavodnik, V. E.; Belskii, V. K.; Zorki, P. M. Crystal Structure of Phenol at 123K. *Zh. Strukt. Khim.* **1988**, *28*, 793–795.

(44) Allan, D. R.; Clark, S. J.; Dawson, A.; McGregor, P. A.; Parsons, S. Pressure-Induced Polymorphism in Phenol. *Acta Crystallogr., Sect. B* **2002**, *58*, 1018–1024.

(45) Das, D.; Banerjee, R.; Mondal, R.; Howard, J. A. K.; Boese, R.; Desiraju, G. R. Synthon Evolution and Unit Cell Evolution during Crystallisation. A Study of Symmetry-Independent Molecules (Z′ > 1) in Crystals of Some Hydroxy Compounds. *Chem. Commun.* **2006**, 555–557.

(46) Kirchner, M. T.; Bläser, D.; Boese, R.; Desiraju, G. R. Additive Induced Polymorphism. The Pentafluorophenol-Pentafluoroaniline System. *CrystEngComm* **2009**, *11*, 229–231.

(47) Gdaniec, M. On the Polymorphs of Pentafluorophenol and Its 2:1 Co-Crystal with Pentafluoroaniline. *CrystEngComm* **2007**, *9*, 286–288.

(48) Thalladi, V. R.; Panneerselvam, K.; Carrell, C. J.; Carrell, H. L.; Desiraju, G. R. Hexagonal Supramolecular Networks in the Crystal Structure of the 1:1 Molecular Complex Trimethylisocyanurate-1,3,5-Trinitrobenzene. *J. Chem. Soc., Chem. Commun.* **1995**, 341–342.

(49) Thallapally, P. K.; Chakraborty, K.; Katz, A. K.; Carrell, H. L.; Kotha, S.; Desiraju, G. R. Matching of Molecular and Supramolecular Symmetry. An Exercise in Crystal Engineering. *CrystEngComm* **2001**, *3*, 134–136.

(50) Thallapally, P. K.; Chakraborty, K.; Carrell, H. L.; Kotha, S.; Desiraju, G. R. Shape and Size Effects in the Crystal Structures of Complexes of 1,3,5-Trinitrobenzene with Some Trigonal Donors: The Benzene-Thiophene Exchange Rule. *Tetrahedron* **2000**, *56*, 6721–6728.

(51) Spackman, M. A.; Jayatilaka, D. Hirshfeld surface analysis. *CrystEngComm* **2009**, *11*, 19–32.

(52) Tan, S. L.; Jotani, M. M.; Tiekink, E. R. T. Utilizing Hirshfeld Surface Calculations, Non-Covalent Interaction (NCI) Plots and the Calculation of Interaction Energies in the Analysis of Molecular Packing. *Acta Crystallogr., Sect. E* **2019**, *75*, 308–318.

(53) Zhao, S.; Kang, L.; Ge, H.; Yang, F.; Wang, C.; Li, C.; Wang, Q.; Zhao, M. Efficient One-Step Synthesis of $C_3$-Symmetrical Benzenoid Compounds Mediated by $SOCl_2$/EtOH. *Synth. Commun.* **2012**, *42*, 3569–3578.

(54) Kotha, S.; Kashinath, D.; Lahiri, K.; Sunoj, R. B. Synthesis of $C_3$-Symmetric Nano-Sized Polyaromatic Compounds by Trimerization and Suzuki-Miyaura Cross-Coupling Reactions. *Eur. J. Org. Chem.* **2004**, 4003–4013.

(55) Wu, X.; Liu, X.; Zhao, G. Catalyzed Asymmetric Aryl Transfer Reactions to Aldehydes with Boroxines as Aryl Source. *Tetrahedron: Asymmetry* **2005**, *16*, 2299–2305.

(56) Pradhan, B.; Pathak, S. K.; Gupta, R. K.; Gupta, M.; Pal, S. K.; Achalkumar, A. S. Star-Shaped Fluorescent Liquid Crystals Derived from s-Triazine and 1,3,4-Oxadiazole Moieties. *J. Mater. Chem. C* **2016**, *4*, 6117–6130.

(57) Ponzini, F.; Zagha, R.; Hardcastle, K.; Siegel, J. S. Phenyl/Pentafluorophenyl Interactions and the Generation of Ordered Mixed Crystals: Sym-Triphenethynylbenzene and Sym-Tris-(Perfluorophenethynyl)Benzene. *Angew. Chem., Int. Ed.* **2000**, *39*, 2323–2325.

(58) Giuglio-Tonolo, A. G.; Spitz, C.; Terme, T.; Vanelle, P. An Expeditious Method for the Selective Cyclotrimerization of Isocyanates Initiated by TDAE. *Tetrahedron Lett.* **2014**, *55*, 2700–2702.

(59) Granovsky, A. A. *FireFly*, version 8; https://www.classic.chem.msu.su/gran/firefly/index.

(60) Schmidt, M. W.; Baldridge, K. K.; Boatz, J. A.; Elbert, S. T.; Gordon, M. S.; Jensen, J. H.; Koseki, S.; Matsunaga, N.; Nguyen, K. A.; Su, S.; Windus, T. L.; Dupuis, M.; Montgomery, J. A. General Atomic and Molecular Electronic Structure System. *J. Comput. Chem.* **1993**, *14*, 1347–1363.

(61) Podolyan, Y.; Leszczynski, J. MaSK: A Visualization Tool for Teaching and Research in Computational Chemistry. *Int. J. Quantum Chem.* **2009**, *109*, 8–16.

(62) Turner, M. J.; McKinnon, J. J.; Wolff, S. K.; Grimwood, D. J.; Spackman, P. R.; Jayatilaka, D.; Spackman, M. A. *CrystalExplorer17*; University of Western Australia, 2017.

(63) Chifotides, H. T.; Dunbar, K. R. Anion-$\pi$ Interactions in Supramolecular Architectures. *Acc. Chem. Res.* **2013**, *46*, 894–906.

(64) Kimura, F.; Oshima, W.; Matsumoto, H.; Uekusa, H.; Aburaya, K.; Maeyama, M.; Kimura, T. Single Crystal Structure Analysis via Magnetically Oriented Microcrystal Arrays. *CrystEngComm* **2014**, *16*, 6630–6634.

(65) Li, Z.-S.; Chen, J.-X.; Huang, Y.-B.; Chen, G.-R.; Lan, T.-Y. 1,3,5-Tris(4-Methylphenyl)Benzene. *Acta Crystallogr., Sect. E* **2006**, *62*, o777–o779.

(66) *International Tables for Crystallography, Volume E: Subperiodic Groups*; Kopský, V., Litvin, D. B., Eds.; Wiley: Chichester, 2010.

(67) Baker, R. J.; Colavita, P. E.; Murphy, D. M.; Platts, J. A.; Wallis, J. D. Fluorine-Fluorine Interactions in the Solid State: An Experimental and Theoretical Study. *J. Phys. Chem. A* **2012**, *116*, 1435–1444.

(68) Rusek, M.; Kwaśna, K.; Budzianowski, A.; Katrusiak, A. Fluorine···Fluorine Interactions in a High-Pressure Layered Phase of Perfluorobenzene. *J. Phys. Chem. C* **2019**, *124*, 99–106.

(69) Thalladi, V. R.; Weiss, H.-C.; Bläser, D.; Boese, R.; Nangia, A.; Desiraju, G. R. C-H···F Interactions in the Crystal Structures of Some Fluorobenzenes. *J. Am. Chem. Soc.* **1998**, *120*, 8702–8710.

(70) Boese, R.; Polk, M.; Bläser, D. Cooperative Effects in the Phase Transformation of Triethylcyclotriboroxane. *Angew. Chem., Int. Ed.* **1987**, *26*, 245–247.

(71) Thalladi, V. R.; Muthuraman, M.; Nangia, A.; Desiraju, G. R. Tri-p-Tolyl-1,3,5-Triazine. *Acta Crystallogr., Sect. C* **1999**, *55*, 698–700.

(72) Mariyatra, M. B.; Panchanatheswaran, K.; Low, J. N.; Glidewell, C. Orthorhombic and Monoclinic Polymorphs of 1,3,5-Triphenylperhydro-1,3,5-Triazine-2,4,6-Trione at 120 K: Chains and Sheets Formed by C-H···$\pi$(Arene) Hydrogen Bonds. *Acta Crystallogr., Sect. C* **2004**, *60*, o682–o685.

(73) Seth, S. K. Structural Characterization and Hirshfeld Surface Analysis of a Co$^{II}$ Complex with Imidazo[1,2-a]Pyridine. *Acta Crystallogr., Sect. E* **2018**, *74*, 600–606.

(74) Baydere, C.; Taşçı, M.; Dege, N.; Arslan, M.; Atalay, Y.; Golenya, I. A. Crystal Structure and Hirshfeld Surface Analysis of (E)-2-(2,4,6-Trimethylbenzylidene)-3,4-Dihydronaphthalen-1(2H)-one. *Acta Crystallogr., Sect. E* **2019**, *75*, 746–750.